Motion control design of the SDSS 2.5 mts telescope

Claudio Rivetta *, Charles Briegel, Paul Czarapata

Fermi National Accelerator Laboratory
P.O Box 500, MS 222, Batavia IL 60510, USA.

ABSTRACT

This paper describes the control system analysis and design for the three principal axes of the 2.5 mts SDSS Telescope. The telescope requirements are good tracking performance with errors lower than 165 marcsec rms in the speed range between 0 to 45 arcsec/sec for all the axes. The pointing error is about 2 arcsec rms per axis with a maximum absolute value of 5 arcsec. The telescope has the additional requirement of slewing, between tracking areas, with maximum speed of 3 degree/sec.

The dynamical model of the telescope including the friction is analyzed and based on that, the design of a PID controller for each axis is presented. The specifications for pointing and tracking mode are achieved with this design in all the range of velocities and the performance in slew-mode is acceptable. Simulations and experimental results depict the behavior of the telescope in slewing, tracking and pointing.

Keywords: *Control system, system modeling, telescopes.*

1. INTRODUCTION

The 2.5 mts SDSS (Sloan Digital Sky Survey) Telescope is designed to accurately track the sky during long periods of time at low speed and slew to different reference points at high speed. The mechanical structure of the telescope is relatively light and resonances appear at frequencies above 12Hz. The telescope has 5 degree of freedom (DOF). Control is performed on azimuth, altitude and instrument rotator axes, while the tilt about the telescope base is restricted by pre-loaded springs acting on four capstans. The motion from DC motors is transmitted to the moving parts by friction capstans. Two motors located diagonally opposite drive the azimuth axis, another two motors move the altitude axis and one motor acts on the rotator. All motors are driven in current mode by linear amplifiers. Axis position is measured using rotary encoders in altitude and azimuth axes and a tape encoder in instrument rotator axis.

The telescope has a wind-screen for protecting against wind perturbations. It covers completely the altitude secondary cage and follows both the azimuth and altitude movements of the telescope. The wind-screen is powered by independent drivers and controlled by a closed loop system to track both the altitude and azimuth axes movements.

The control system is divided in three operative blocks. The telescope control computer (TCC), the motion control processor (MCP) and the telescope axis control. The TCC is the trajectory generator and the operator interface. Based on astrometrical considerations, this subsystem generates the trajectory to follow on the sky by the telescope in both tracking and slew mode. The TCC sends to the MCP 'triplets' composed by the *position* and *velocity* and the *time* at which those values are required. These triplets are not evenly spaced in time.

---

* *On leave of absence from Fermilab. Now with ETH Zurich / CERN, Switzerland.*
Correspondence to: rivetta@fnal.gov , Claudio.Rivetta@cern.ch

The MCP is implemented with a VME general-purpose processor and a multi-axis controller. It performs the control algorithm for the three principal axes, generates the reference for each axis based on the TCC triplets, monitors the principal variables per axis and interfaces the control system with the interlock system.

This paper is organized as follow, in section 2 a brief description of the system is presented. Section 3 describes the MCP implementation, section 4 presents the considerations followed in the closed-loop design and some simulation results and, finally, section 5 depicts experimental results.

2. SYSTEM DESCRIPTION

The block diagram of the system is shown in figure 1. The telescope control computer (TCC) is resident in a Compaq VMS Alpha computer. It is the trajectory generator and the interface with the operator. This remote computer sends the information to the motion control processor (MCP) using a 9600 baud RS232 link.

The MCP is based on both a VME general processor (MVME162) and a VME multi-axes controller (MEI). The MVME162 module interfaces the control system with the TCC, the interlock system and the telescope performance monitor (TCP). In combination with the MEI, this module performs the control algorithm for the three principal axes, generates the reference for each axis based on the TCC information and monitors the principal variables per axis. The MEI is a six independent axis controller based on a PID algorithm. Also, it includes an internal routine capable of generating the reference trajectory for each axis using a 2nd order interpolation.

The output signal from the MEI controller is filtered and acts as reference for the current amplifiers that drive the DC electric servo-motors. All the axes use similar servo-motors coupled to the disk drive by friction capstans. Two motors diagonally opposed drive the azimuth axis, two motors drive the altitude axis and one motor drives the instrument rotator. Optical encoders measure the position on each axis and feedback the signal to the MEI controller. Encoders attain the resolution required by using interpolators.

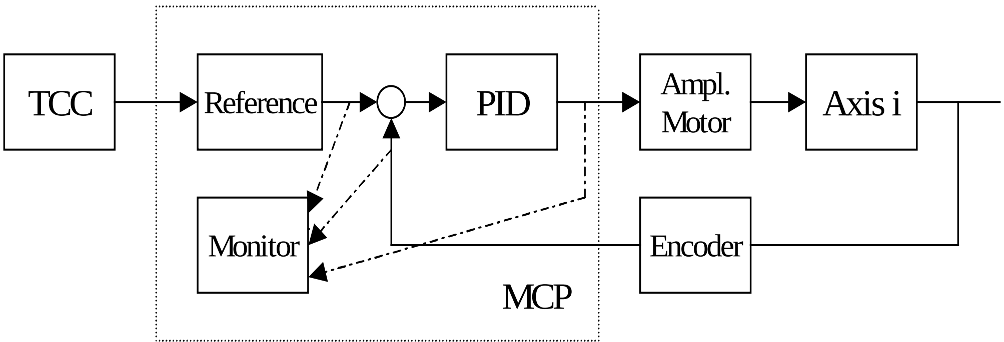

Figure 1.- Block diagram of control system.

3. MOTION CONTROL PROCESSOR (MCP)

The TCC combines both the trajectory generation for the three axes and the interface with the operator. This interface includes different functions as braking, some instrument accessories, fidutial resetting, etc. More information about the TCC features can be found in the SDSS web site [1]. Based on astrometrical considerations, the TCC generates the trajectory using a 3rd degree polynomial. Each sector is interpolated based on a constant jerk algorithm. The TCC sends to the MCP triplets composed by the position, velocity and time for each axis. These triplets are sent in advance to the real position of the telescope. They define the future position and velocity that the telescope has to reach at the specified time. Those triplets are sent at irregular time.

Based on that information, the MCP has to generate the reference for each axis at a regular sampling. The MEI, the processor that performs the control, has an internal routine for trajectory generation based on a 2nd order interpolation. If the trajectory is generated directly using the TCC triplets large error are induced due to the different methods of interpolation. In order to approximate the original trajectory with minimum error, it is re-sampled at a regular period of 50 msec by the VME general processor. The new reference points are interpolated using the 2nd order polynomial routine included into the MEI controller. This operation is described in figure 2. The sampling frequency of the reference input is equal to the closed-loop switching frequency, that is 160Hz. This procedure is used if the telescope is either tracking or slewing in the sky.

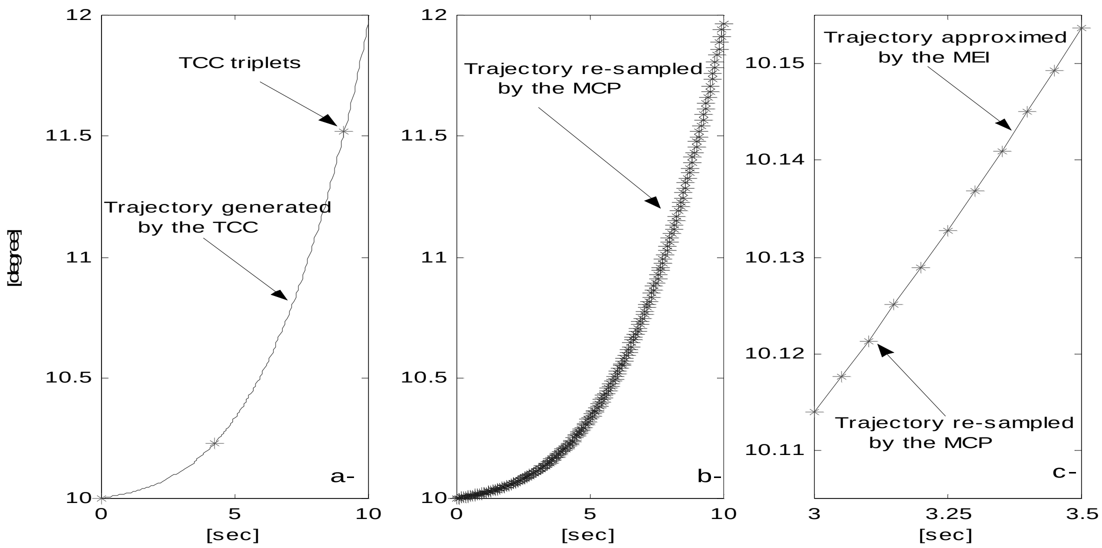

Figure 2 .- a) Trajectory generated by the TCC and triplets sent to the MCP.-
b) Trajectory re-sampled by the MCP using the original 3rd order polynomial.
c) Trajectory approximated by the MEI using the 2nd order polynomial, based on the re-sampled points.

The control of each axis is performed by a proportional-integral-derivative (PID) algorithm resident into the MEI controller. The parameters for each loop are the same for both modes of operation, tracking and slewing. It simplifies substantially the system because it is not necessary to switch parameters when the telescope changes the operation mode. Under this design the telescope operates continuously from zero velocity up to maximum speed in slewing mode. The design of the closed-loop is further described in another section.

Optical encoders measure the position on each axis. Altitude and azimuth axes use two relative rotational encoders located diagonally on the disc surface. In order to get an absolute position, a fidutial system is used. It is composed by pieces of tape encoder spaced regularly around the disk surface of each axis and a read head to collect the reference signal of each piece of tape. Each tape is identified using an UPS bar code system on the azimuth or the clinometer output voltage for the altitude angle. The Instrument Rotator uses a tape encoder with four read heads. At the moment, two heads are used in the system due to limitations imposed by the MEI controller to read out the four heads. One of the heads reads the tape marks as a relative encoder and the other reads the absolute marks or references. A digital circuit is used to interface the reference signals with the MCP. It generates interruption to both the MEI controller and the MVME 162 based on the reference signal. Due to the interruption, the MEI latches the values read from all the relative encoder. The MCP discriminates which axis hits the reference mark and stores the read value to calculate the absolute position.

A fixed set of variables for each axis can be collected by the MCP at 33Hz (maximum 100Hz for one axis). The MCP stores these values and other important information from the telescope into the dual-ported memory on the VME bus. The Telescope Performance Monitor (TCP) is a similar processor as the MCP and archives the user-specified subset of this data to disk. This archive can be retrieved off-line for diagnostic and monitoring. More information about this feature can be found at the SDSS web site [2].

4. CLOSED-LOOP DESIGN

The telescope requirements are good tracking performance with errors less than 165 marcsec rms for time scales between 1 and 10 minutes for altitude and azimuth axes and less than 100 marcs rms for time scales shorter than 1 minute. The instrument rotator requirements are less exigent, it is tolerated errors up to 500 marcs rms. These tracking specifications have to be verified in the speed range between 0 to 45 arcsec/sec for all the axes. The pointing error is about 2 arcsec rms per axis with a maximum absolute error of 5 arcsec . The telescope has the additional requirement of slewing, between tracking areas, with maximum speed of 3 degree/sec.

The criterion to follow in the design is to achieve the performance specification with a controller topologically simple, with a simple algorithm and a maximum band-width to improve the rejection to external perturbations. These goals are opposite each other and some compromise has to be achieved to satisfy the specifications and a simple implementation.

The system presents a hard-non linearity due to the friction. There is not direct method to calculate the controller parameters based on both the system specifications and stability. To simplify the controller design the rigid model of the telescope is used. Under this assumption, the bandwidth can not be increased without compromising the stability due to the high frequency dynamics non-modeled. In low frequency, it is necessary to contemplate the friction effect and limitations that it introduces in the design. In order to describe those limitations, a brief analysis of the structure and the bearing friction as well as its mathematical model is included.

a) Structure model – Rigid Model

The telescope is a light mechanical structure with resonances above 12 Hz. It corresponds to a torsional resonance of the altitude secondary cage. Since the control is performed only on three axes, the analysis is performed considering the telescope as a 3 DOF structure. A rigid model is used to mathematically describe the dynamic behavior of the telescope. The model can be written as:

$$M(\theta)\cdot\frac{d^2\theta}{dt^2}+V(\theta,\frac{d\theta}{dt})+G(\theta)+T_f(t)+T_{disturbances}=T \qquad (1)$$

where:

$\theta = [\theta_1\ \theta_2\ \theta_3]^{\mathbf{T}}$: Position of reference axis of joints 1,2 and 3. (3x1 vector), ([..]**T** denotes transpose)

$T = [T_1\ T_2\ T_3]^{\mathbf{T}}$: Mechanical torque applied to the structure by the capstans. (3x1 vector)

$M(\theta)$: Mass matrix. (3x3 matrix)

$G(\theta)=[G_1\ G_2\ G_3]^{\mathbf{T}}$: Gravity vector (3x1 vector)

$V(\theta, \frac{d\theta}{dt})$: Centrifugal and Coriolis vector. (3x1 vector)

$T_f(t)$: Friction torque on joints 1,2 and 3.

$T_{disturbances}$: Disturbance torque (wind disturbance, etc.) (3x1 vector)

The parameters or elements of the matrices M(θ), C(θ), B(θ) and G(θ) can be derived mathematically using solid model analysis. DC motors driven in current mode and coupled directly to the structure by friction capstans generate torques T1, T2 and T3, corresponding to azimuth, altitude, and instrument rotator axes, respectively. Mathematically, each torque can be expressed as:

$$T_i = n_m . n_c . K_T . i_{ref} \qquad i = 1, 2, 3 \tag{2}$$

where:

nc = ratio between the capstan diameter and azimuth / altitude / rotator disc diameter.

Kt = Torque constant.

iref = Motor current.

nm = number of motors driving each axis (nm = 2 for azimuth, altitude, nm = 1 for rotator)

The term $V(\theta, \frac{d\theta}{dt})$ and the coupling terms of M(θ) can be neglected assuming low-velocity and low-acceleration operation. In that case, a simplified de-coupled structure can be considered in the design. Entries of G(θ) are equal to zero if the corresponding link is in balance. This should be the ideal case for all of them but altitude axis is unbalanced during the operation. It is due to the change of liquid nitrogen level of intermediate dewars used to refrigerate the mosaic camera and spectrographs.

b) Friction Model

The most important non-linearity in the system is the bearing friction of each axis. Mathematical models that describe the behavior of the friction at high and low speed have been presented in the literature [3] [4]. In a previous paper [5], the *LuGre* model is analyzed and used to describe the friction of the principal axes of this telescope. The model incorporates both the dynamic behavior in the striction and low speed region and the static behavior of the friction when the axis moves a constant velocity. The dynamic behavior of the friction is captured by an internal state that can be interpreted as the average deflection of the surface bristle of the metallic parts in contact. The friction torque can be mathematically represented as:

$$T_f(t) = \sigma_o . z + \sigma_1 . \frac{dz}{dt} + \sigma_2 . v \tag{3}$$

where v is the relative velocity between the two surfaces, z is the average deflection of bristles, σ_o a stiffness coefficient, σ_1 a damping coefficient and σ_2 is the viscous coefficient. The dynamic of the average bristle deflection can be expressed as:

$$\frac{dz}{dt} = v - \frac{|v|}{g(v)} . z \tag{4}$$

The first term points the deflection is proportional to the integral of the relative velocity. The second is included to make the deflection converge to the value

$$z_{ss} = g(v).\mathrm{sgn}(v) \tag{5}$$

under steady state conditions (v = constant). In steady state (constant velocity), the friction torque is described as:

$$T_{fss}(v) = \sigma_o . g(v).\mathrm{sgn}(v) + \sigma_2 . v \tag{6}$$

where the $\sigma_0.g(v)$ function have been proposed to model the steady-state friction-velocity mapping [3] [4] . If $\sigma_0.g(v)$ take into account the Striebeck effect and the Coulomb friction, the steady state friction torque is:

$$T_{fss}(v) = [Tc + (Ts - Tc).e^{-(v/vs)^2}].\mathrm{sgn}(v) + \sigma_2.v \qquad (7)$$

where Ts is the level of static friction, Tc is the Coulomb friction and v_s is an empirical parameter. The *LuGre* model is continuous and admits a unique solution, given an initial condition, due to its Lipschitz properties.

In the literature several methods have been presented to control mechanical systems with friction. They include adaptive compensation of the friction, non-linear observers and neural networks [6] [7] [8]. They are characterized by injecting, as a feed-forward signal, an estimation of the friction torque. It compensates the effect of the friction, leaving an equivalent mechanical system without the friction perturbation. This methodology complicates the controller algorithm and it is not used in this design.

There are, also, some analysis that includes the friction perturbation into the design of controllers based on more simple algorithms [9] [10] [11]. It has been shown in [12] using singular perturbation approach, for unidirectional cases, that it is possible to consider the friction term as the steady-state friction plus a term dependent of the bristle deflection. They have shown the last term is only important at low-speed and increasing accelerations. In the controller design, it is necessary to increase the proportional and derivative terms of the PID to stabilize the system perturbed by friction. The criterion used to set the PID coefficients was to shape the open-loop response to achieve good performance and stability and to limit the high frequency response to avoid high frequency oscillations.

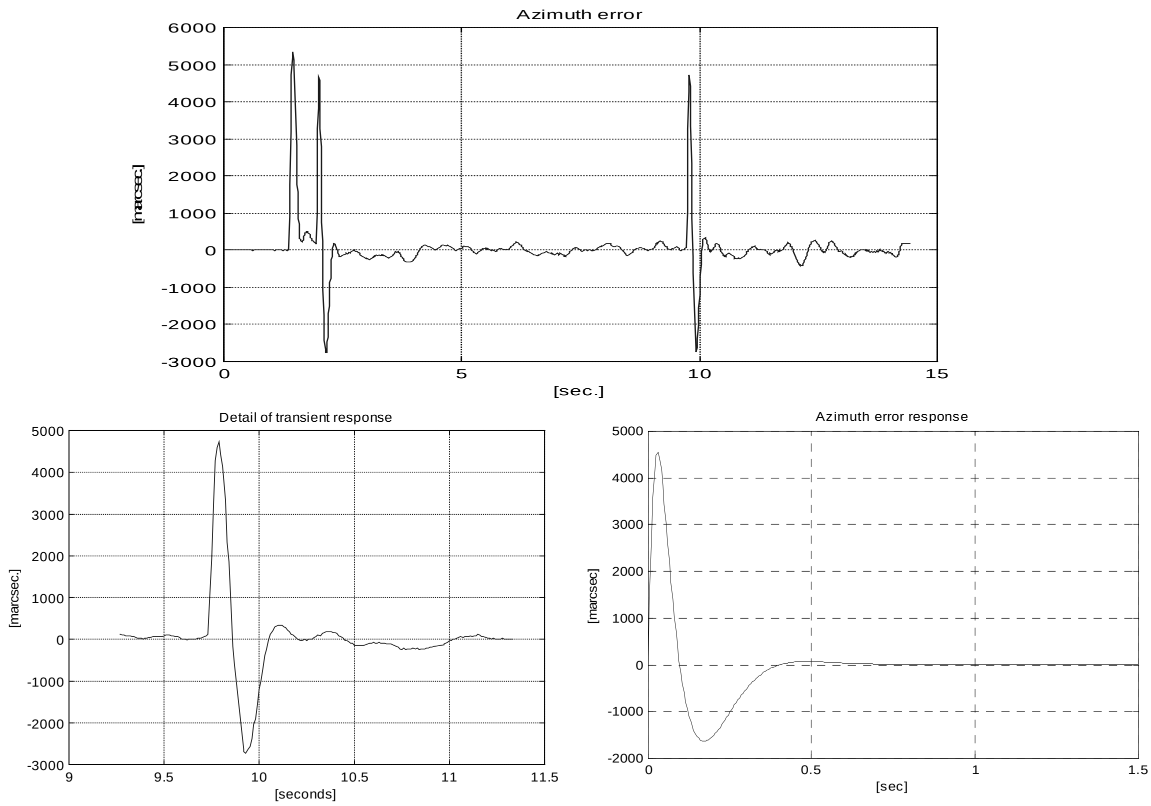

Figure 3. a) Position error response of the azimuth axis to steps in velocity (144 arcsec/sec)
b) Detail of error response
c) Response obtained by simulation.

The MEI controller uses a PID algorithm with fix point representation. It approximates the integral and derivative using backward differences. External low-pass filters where included into the power amplifiers to shape the high frequency open loop response and avoid high frequency oscillations. The present controller introduces several limitations in the design that does not allow setting the maximum gain in the encoder interpolators. The actual resolution values are 14.4 marcsec/count for altitude and azimuth axes and 21 marcsec/count for the instrument rotator axis. These limitations are due to the fix point representation, the maximum integral value, and the minimum sampling frequency.

The parameters obtained following this method were finally adjusted on the telescope using as a test driving signal steps in velocity with limited acceleration. The error response of the telescope under this driving signal is depicted in figures 3 and 4. Each axis is moved from zero velocity toward increasing velocities following sequential velocity steps of 144 arcsec/sec. Figures 3b and 3c depict the real response of azimuth axis to this signal and the response obtained by simulation, respectively. Figures 4b and 4c show similar results for the altitude axis.

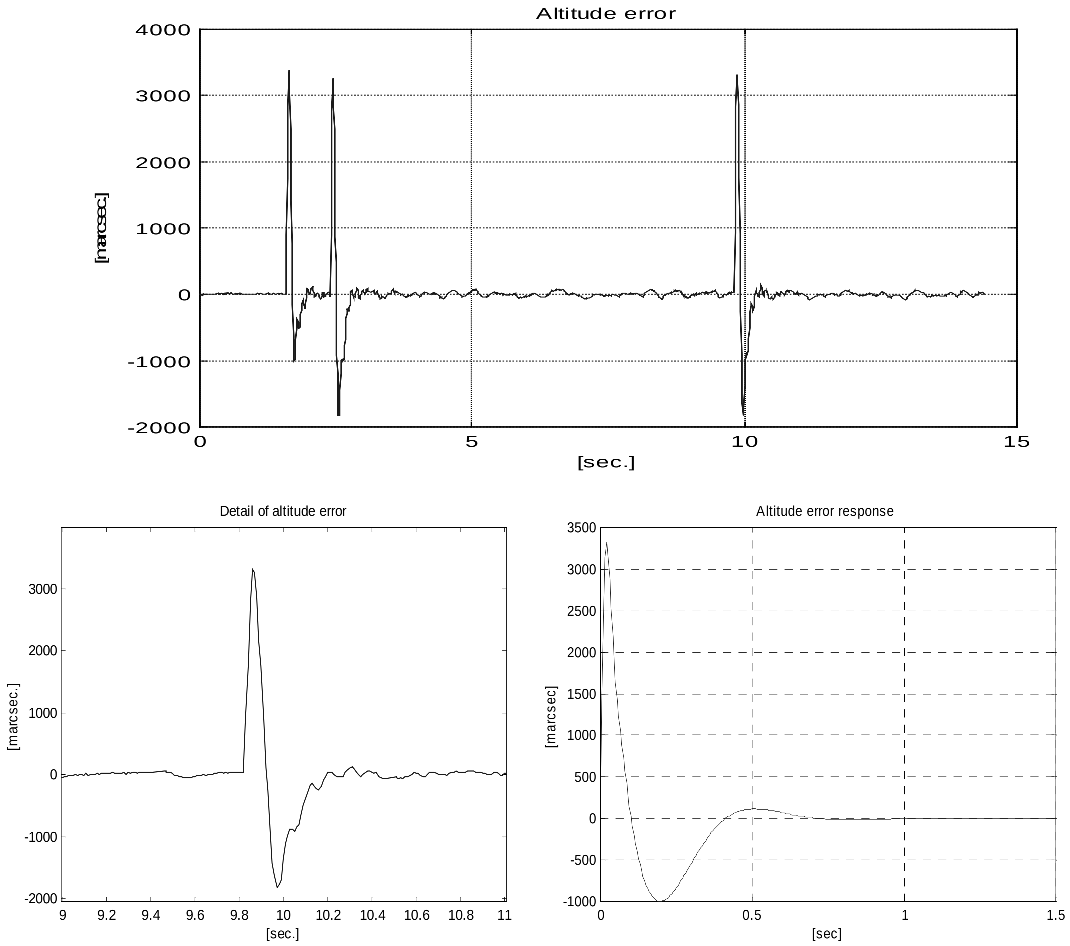

Figure 4. a) Position error response of the altitude axis to steps in velocity (144 arcsec/sec)
b) Detail of error response
c) Response obtained by simulation

5. PERFORMANCE

To show the performance of the telescope operating under different modes, several plots collected with the MCP acquisition system are shown. During the acquisition, the mean value of the wind speed was about

10 -15 mph (17 - 25 km/hr). Figures 5 and 6 show the performance of azimuth and altitude axes when the telescope is tracking on the sky. The RMS value of the error calculated during an interval of 11 sec is, in all the cases, lower than the specified value. On the azimuth error, the negative 'spikes' are due to coupling between the telescope and the wind-screen structure.

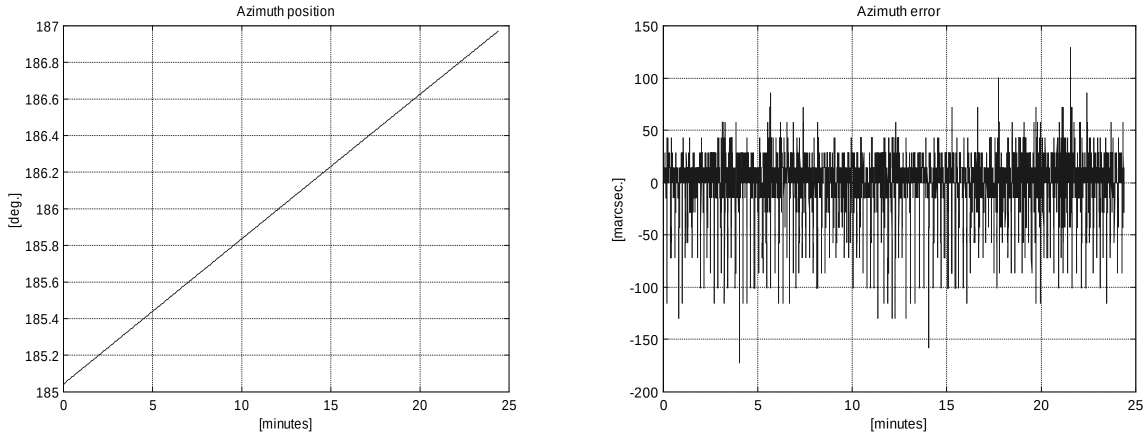

Figure 5. Absolute position and position error of the azimuth axis during tracking.

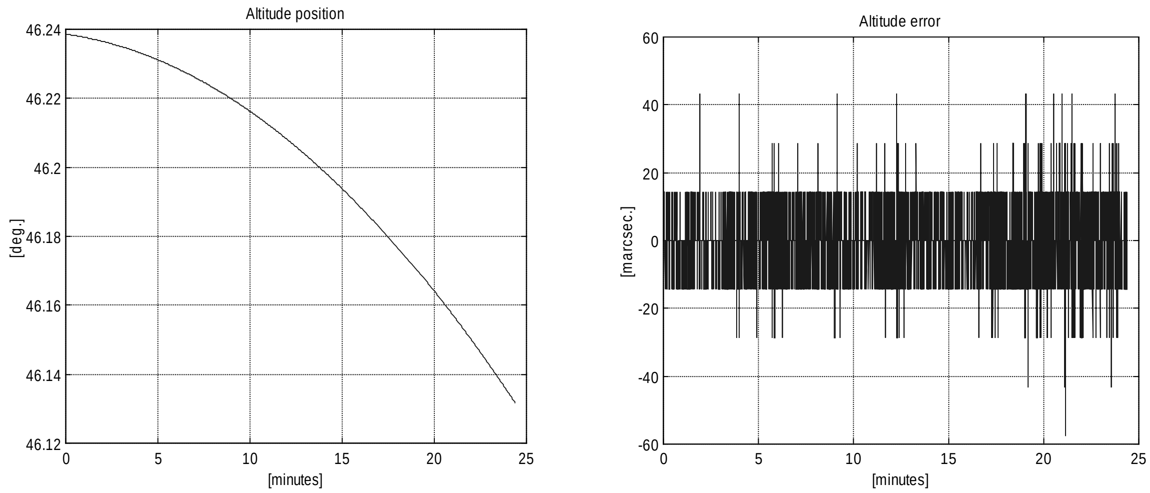

Figure 6. Absolute position and position error of the altitude axis during tracking.

Figure 7 depicts the performance of the telescope when it is pointing an object at 45 degree in altitude. The slewing performance is shown in figure 8. In this case the telescope is commanded to move in azimuth from 0 degree to 140 degrees and return to home position at maximum speed. In this case the telescope accelerates up to reach the maximum speed, performs the trajectory at such a speed and then decelerates up to reach the new position. It holds at 140 degrees during 10 seconds and returns to 0 degree at maximum speed.

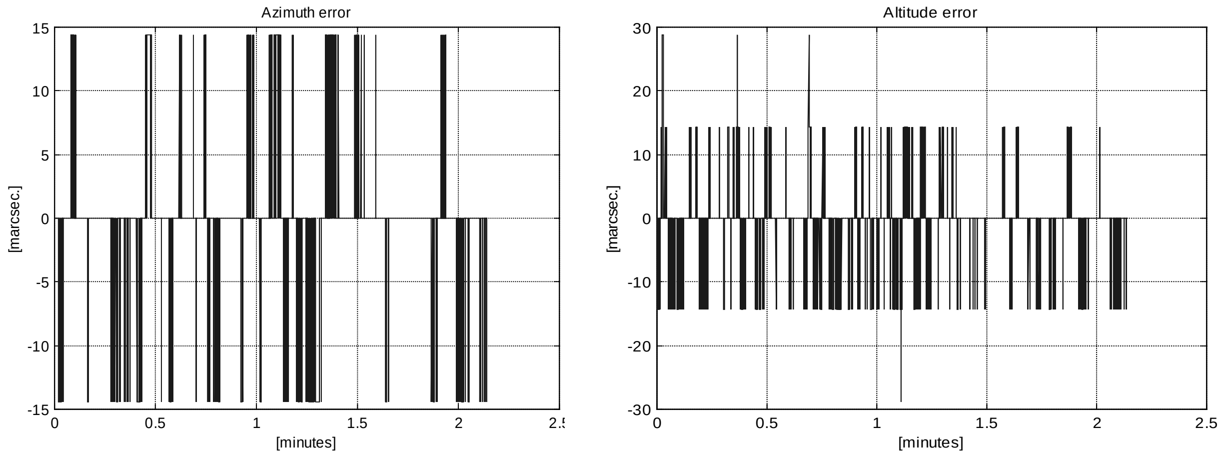

Figure 7. Azimuth and altitude axes pointing errors (Altitude axis ≅ 45°)

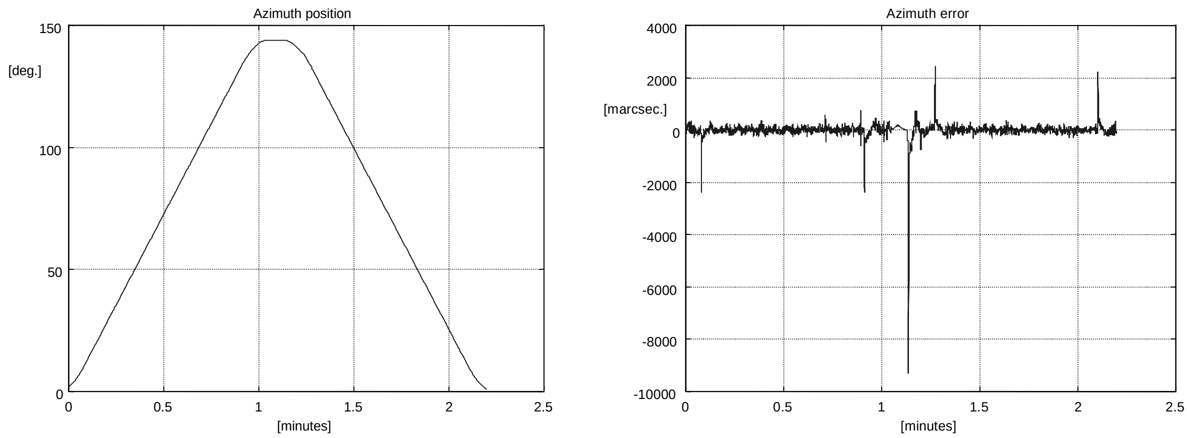

Figure 8. Azimuth axis slewing performance. Absolute position from 0° to 140° and return to 0°

6. CONCLUSION AND FUTURE WORK

In this paper, the description and performance of the 2.5 mts telescope servo-system has been presented. The servo-control fulfills the requirements using both a simple topology and a PID strategy. The telescope is able of pointing and tracking on the sky with errors lower than the specified values and the performance during slewing mode is acceptable. A particular advantage of this design is each telescope axis can move from zero velocity to maximum speed without neither switching algorithms nor changing parameters in the controller. Some improvements should be implemented before the final commissioning test. It should include an enhancement of the position read-out of the instrument rotator, a better strategy of anti-reset wind-up in the controller and an improvement in the coupling between wind-screen and telescope.

ACKNOWLEDGES

The authors would like to acknowledge to William Borosky for the coordination of the work performed at APO, French Leger for the support and help during the development and adjustment of the servo-system, James Gunn and Robert Nagel for the fruitful discussions and guidness. They would like, also, to thanks to the SDSS collaboration and APO personal for the support and help. This work was supported by the U.S. Department of Energy under contract No. DE-AC02-76CH03000.

REFERENCES

1. R. Owen, " TCC Documentation " http://www.apo.nmsu.edu/Telescopes/

2. R. Neswold, " Telescope Performance Monitor " http://tdpc01.fnal.gov/sdss/project.htm

3. C. Canudas de Wit, H. Olsson, K. Astrom, P. Lischinky, "A New Model for Control of System with Friction," *IEEE transaction on Automatic Control.* **40**, pp. 419-425, March 1995.

4. B. Armstrong-Helouvry, P. Dupont, and C. Canudas de Wit, " A survey of models, analysis tools and compensation methods for the control of machines with friction," *Automatica* , **30,** pp.1083-1138, 1994.

5. C. Rivetta, S. Hansen, "Friction Model of the 2.5mts SDSS Telescope," *SPIE International Symposium of Astronomical Telescopes and Instrumentation.* **Vol. 3351** March 1998. Also, *FERMILAB-CONF-98-070*, February 1998

6. R. Hirschorn, G. Miller, "Control of Nonlinear Systems with Friction," *IEEE Transaction on Control Systems Technology.* **7, no.5,** pp. 588-595, September 1999.

7. N. Leonard, P. Krishnaprasad, "Adaptive Friction Compensation for Bi-directional Low-Velocity Position Tracking," *Proc. 31st Conference on Decision and Control*, pp. 267-273, December 1992.

8. P. Vedagarbha, D. Dawson, M. Feemster, " Tracking Control of Mechanical Systems in the Presence of Nonlinear Dynamic Friction Effects" *IEEE Transaction on Control Systems Technology.* **7, no.4,** pp. 446-456, July 1999.

9. S. Huang, J. Yen, "Dual Mode Control of a System with Friction," *IEEE Transaction on Control Systems Technology.* **7, no.3,** pp. 306-314, May 1999.

10. P. Dupont, E. Dunlap, "Friction Modeling and PD Compensation at Very Low Velocities," *Transaction of the ASME, Journal of Dynamic Systems, Measurement, and Control.* **Vol. 117,** pp. 8-14, March 1995.

11. P. Dupont, "Avoiding Stick-Slip Through PD Control" *IEEE transaction on Automatic Control.* **39,no.5**, pp. 1094-1097, May 1994.

12. F. Altpeter, F. Ghorbel, R. Longchamp, "Relationship Between Two Friction Models: A Singular Perturbation Approach" *Proc. 37th. Conference on Decision and Control,* pp. 1572-1574, December 1998.